CMB radiation in an inhomogeneous spherical space

R. Aurich[1], P. Kramer[2] and S. Lustig[1]

[1]Institut für Theoretische Physik, Universität Ulm,
Albert-Einstein-Allee 11, D-89069 Ulm, Germany
[2]Institut für Theoretische Physik der Universität,
Auf der Morgenstelle 14, D-74076 Tübingen, Germany

Abstract. We analyse the CMB radiation in spherical 3-spaces with non-trivial topology. The focus is put on an inhomogeneous space which possesses observer dependent CMB properties. The suppression of the CMB anisotropies on large angular scales is analysed with respect to the position of the CMB observer. The equivalence of a lens space with a Platonic cubic space is shown and used for the harmonic analysis. We give the transformation of the CMB multipole radiation amplitude as a function of the position of the observer. General sum rules are obtained in terms of the squares of the expansion coefficients for invariant polynomials on the 3-sphere.

PACS numbers: 98.80.-k, 98.70.Vc, 98.80.Es

Submitted to: *Phys. Scr.*

1. Introduction.

Cosmic topology examines multi-connected manifolds as candidates for the spatial part of cosmic space-time. It simulates the cosmic microwave background (CMB) radiation using the eigenmodes of the multi-connected manifolds, and explores if the specific multipole amplitudes and selection rules arising from the manifold are encoded in the CMB radiation.

In this paper the focus is put on spherical spaces. The simply connected 3-sphere underlies Einstein's initial cosmological analysis of 1917 [9]. In that year de Sitter [35] already discussed the projective space $\mathbb{P}^3$ as an alternative to Einsteins model. This was the first cosmological application of a spherical model which is multiply connected, i. e. being a closed three-dimensional piece of Einstein's 3-sphere.

The topology of a manifold $\mathcal{M}$ is locally described by homotopy. Homotopy composes loops on the manifold by concatenation and explores the homotopy group $\pi_1(\mathcal{M})$ formed by these loops. If any loop can be continuously contracted to a point, the manifold is simply connected. Any topological manifold has an image on a simply connected covering manifold. The covering manifold $\tilde{\mathcal{M}}$ is tiled by copies of $\mathcal{M}$. Covering manifolds and their tiles can be spherical, Euclidean or hyperbolic. In terms

of the Riemannian metric they display constant positive, zero or negative curvature. In this paper, we concentrate on spherical manifolds which tile the 3-sphere $\mathbb{S}^3$.

The second concept of a cover offers a global and quasi-crystallographic view of a topological manifold. On the covering manifold $\tilde{\mathcal{M}}$ there is a group deck($\mathcal{M}$) of deck transformations which by fix-point free action tiles the covering manifold. Seifert and Threlfall [36] show that the two groups are isomorphic, $H = \text{deck}(\mathcal{M}) \sim \pi_1(\mathcal{M})$, and so the first local and the second global view of topology, in terms of the group H as topological invariant, are equivalent.

In an abstract approach, a topological manifold is taken as a quotient space $\tilde{\mathcal{M}}/H$ of the covering manifold $\tilde{\mathcal{M}}$ by the group H. If this notion refers to the abstract group and not to a representation thereof, it leaves open the geometric form of the manifold. An algebraic characterisation for the classification of spherical space forms is given by Wolf [43] in terms of unitary matrix representations of groups H, acting on the 3-sphere.

An introduction into the topological concept applied to the cosmological framework can be found in [24, 28] where all three spatial curvatures are discussed. The focus was shifted to spherical spaces [11] by the paper [29] which claims that the low power in CMB anisotropies at large scales can be described by the Poincaré dodecahedral topology. Thereafter, a lot of papers discussed the relevance of this result, and other spherical spaces such as the truncated cube and the tetrahedral space were investigated with respect to their statistical CMB properties, see e. g. [33, 12, 1, 2, 3, 30, 34]. In addition, spherical lens spaces $L(p, q)$ are studied in [39]. The fundamental domain can be visualised by a lens-shaped solid where the two lens surfaces are identified by a $2\pi q/p$ rotation for relatively prime integers p and q with $0 < q < p$. For more restrictions on p and q, see below and [11]. A further family of spherical spaces, the so-called Platonic polyhedra, were constructed from their homotopy groups and studied in [16, 21, 22, 23].

In the present paper, we examine the equivalence of spherical manifolds, the observer dependence of the multipole expansion, and quadratic sum rules following from the reduction of representations. We show the equivalence of the Platonic cubic manifold $N2$ and the lens manifold $L(8, 3)$ and investigate the statistical properties of CMB anisotropies. The geometry of the manifold can be expressed by the Voronoi domain (see below) which has the observer of the CMB radiation in its centre. It turns out that the Platonic cubic geometry of the manifold $N2$ is equivalent to a special observer position in the manifold $L(8, 3)$. This manifold is not homogeneous and is thus called inhomogeneous. In order to emphasise this point, consider two observers where the first observer position can be mapped by a transformation M onto the second one. Assume that the first observer determines his Voronoi domain by the group elements $g \in H$, then the second observer gets his Voronoi domain by the group MgM^{-1}. That is a similarity transformation, or a coordinate transformation. If M and g commute for all $g \in H$, then both observers see the same Voronoi domain. In this case, one has a homogeneous manifold. On the other hand, if M and g do not commute, one obtains observer dependent Voronoi domains and thus an inhomogeneous manifold. The interesting point of view with respect to cosmic topology is that the statistical

properties of the CMB radiation is observer dependent in the inhomogeneous case. As two examples for homogeneous manifolds, we also analyse the lens space $L(8,1)$ and the Platonic cubic manifold $N3$. The latter is equivalent to a manifold generated by the binary dihedral group D_8^* isomorphic to the quaternion group Q.

2. Specification and equivalence of spherical manifolds with volume $V(\mathbb{S}^3)/8$.

The geometry of a spherical manifold is not determined by a quotient $\mathbb{S}^3/H$ if its deck group H is only specified by its group relations. Once we have identified a group H and its action on the 3-sphere for two geometric shapes, we only know that both shapes may serve as fundamental domains under H acting on the cover. A fundamental domain for H is a subset of points on the cover such that no element of $g \in H,\ g \neq e$ can operate inside the domain, but any point of the cover outside the domain can be reached by the action of H on a point inside the domain. The fundamental domain $\mathcal{F}$ with respect to the position x_o of the observer is defined to be the set of points x which satisfy

$$d(x_o, x) \ \leq \ d(x_o, g(x)) \ \ \forall \ \ g \in H \quad , \tag{1}$$

where $d(x, x')$ is the distance between the points x and x'. A fundamental domain constructed in this natural way is called Voronoi domain. For historical reasons, there are several other names for such a domain in use, for example the Dirichlet cell, see [31], but we use Voronoi in the following.

How can we find out if two spherical manifolds are equivalent under homotopy? The example of two cubic spherical manifolds shows that, even for equal geometric shape of the fundamental domain, their topologies, encoded in their homotopic boundary conditions, can be inequivalent, i. e. they can possess different deck groups. Homotopic equivalence requires to find a one-to-one map between the two geometric shapes which reproduces the homotopic boundary conditions. We demonstrate homotopic equivalence on the Platonic cubic manifold $N2$ from [21] versus the lens spherical manifold $L(8,3)$, see [36] p. 210.

Let us now turn to the specification of spherical manifolds with volume $V(\mathbb{S}^3)/8$, i. e. manifolds generated by groups having 8 elements. There are two lens spaces $L(p,q)$ with order 8, since p and q have not only to be relatively prime with $1 \leq q < p$. The spaces $L(p,q)$ and $L(p',q')$ are homeomorphic if and only if $p = p'$ and either $q = \pm q' (\mathrm{mod}\ p)$ or $q\,q' = \pm 1 (\mathrm{mod}\ p)$ [11]. For example, the lens spaces $L(p,q)$ and $L(p,p-q)$ are mirror images. These restrictions leave as representations of the cyclic group C_8 only the lens spaces $L(8,1)$ and $L(8,3)$, where the former is a homogeneous and the latter an inhomogeneous manifold. A further manifold generated by a group of order 8 corresponds to the binary dihedral group D_8^*, isomorphic [19] to the quaternion group Q, and admits the cubic Platonic manifold $N3$. The lens manifold $L(8,3)$ is equivalent to the Platonic cubic manifold $N2$. This completes the list of manifolds with volume $V(\mathbb{S}^3)/8$.

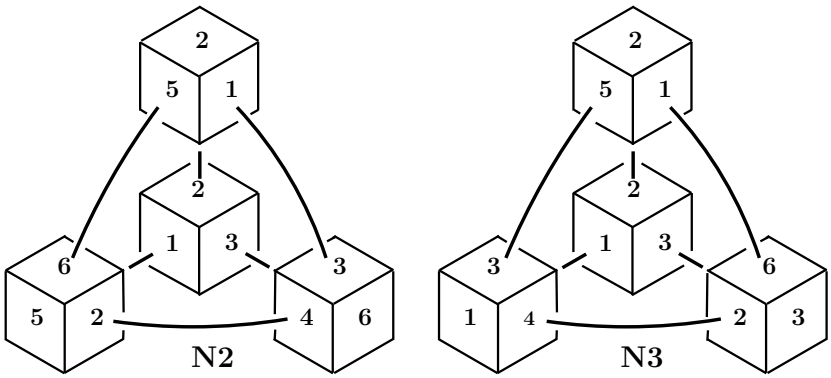

Figure 1. The cubic manifolds $N2$ and $N3$. The cubic prototile and three neighbour tiles sharing its faces $F1, F2, F3$. The four cubes are replaced by their Euclidean counterparts and separated from one another. Visible faces are denoted by the numbers in eq. (2). The actions transforming the prototile into its three neighbours generate the deck transformations and the 8-cell tiling of $\mathbb{S}^3$. In the tiling, homotopic face gluing takes the form of shared pairs of faces $N2 : F3 \cup F1, F4 \cup F2, F6 \cup F5$ and $N3 : F1 \cup F6, F2 \cup F4, F3 \cup F5$. It is marked by heavy lines or arcs.

2.1. The cubic spherical manifolds $N2$ and $N3$.

There are two inequivalent Platonic cubic spherical manifolds $N2$ and $N3$ [21], with homotopy groups derived in [10]. Their gluing is shown in figure 1. First we consider the gluing of the spherical cube which leads to the manifold $N2$.

Face gluings N2: After correction of an error in [19] eq. (9), we have from [21]

$$N2 : \; F3 \cup F1, \; F4 \cup F2, \; F6 \cup F5. \tag{2}$$

Edge gluing scheme N2: Directed edges in a single line in eq. (3) are glued. A bar over an edge number means that the direction of the edge is reversed before the gluing.

$$N2 : \begin{bmatrix} 1 & 3 & 4 \\ 2 & 6 & \overline{9} \\ 5 & 7 & \overline{10} \\ 8 & 11 & \overline{12} \end{bmatrix} \tag{3}$$

The elements of the rotation group

$$\mathrm{SO}(4,\mathbb{R}) \sim (\mathrm{SU}^l(2,\mathbb{C}) \times \mathrm{SU}^r(2,\mathbb{C}))/\{\pm(e,e)\} \tag{4}$$

are denoted as pairs (g_l, g_r). They act on the points $u \in \mathrm{SU}(2,\mathbb{C})$ of the 3-sphere $\mathbb{S}^3 \equiv \mathrm{SU}(2,\mathbb{C})$ by

$$(g_l, g_r) : u \to g_l^{-1} u g_r. \tag{5}$$

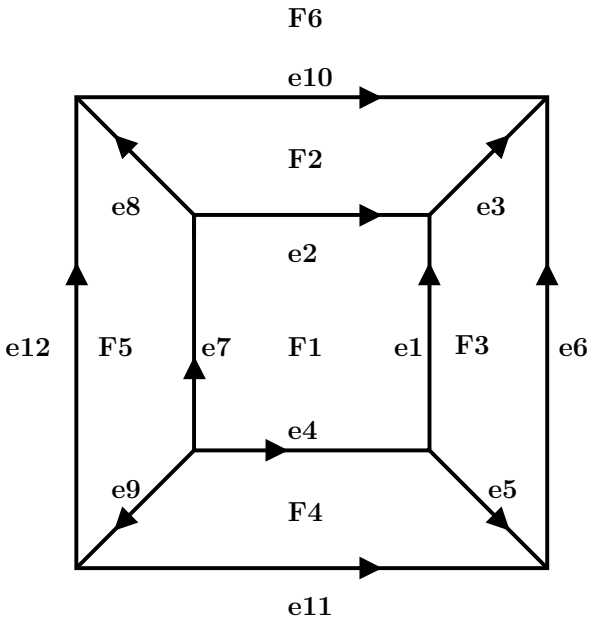

Figure 2. A sketch to explain the gluing of the faces (Fi) and the edges (ei) of the spherical cubic manifolds $N2$ and $N3$.

Group H = deck($N2$): Another description of this manifold is given by the identification of the points on the covering space $\mathbb{S}^3$ by the group $H = \mathrm{deck}(N2)$ which is the cyclic group C_8 generated by the element (an irrelevant minus sign in [21] has been dropped)

$$g := (g_l, g_r) = \left(\begin{bmatrix} \overline{a} & 0 \\ 0 & a \end{bmatrix}, \begin{bmatrix} 0 & a^3 \\ a & 0 \end{bmatrix} \right) \tag{6}$$

with $a = \exp(2\pi \mathrm{i}/8)$, and $g_l, g_r \in \mathrm{SU}(2,\mathbb{C})$. Then the corresponding manifold is invariant under

$$u \to u_n = \left(g_l^{-1}\right)^n u \, (g_r)^n \ , \ \ n = 1,..,8 \tag{7}$$

of all points

$$u = \begin{bmatrix} z_1 & z_2 \\ -\overline{z}_2 & \overline{z}_1 \end{bmatrix} = \begin{bmatrix} x_0 - \mathrm{i}x_3 & -x_2 - \mathrm{i}x_1 \\ x_2 - \mathrm{i}x_1 & x_0 + \mathrm{i}x_3 \end{bmatrix} \in \mathrm{SU}(2,\mathbb{C}) \equiv \mathbb{S}^3 \quad . \tag{8}$$

Transcribing the same action of this group C_8 into real notation we get

$$\vec{x} = (x_0, x_1, x_2, x_3)^T \in \mathbb{S}^3 \to \vec{x}_n = (R_g)^n \ \vec{x} \ , \ \ n = 1,..,8 \tag{9}$$

with the generator of the group

$$R_g = \begin{bmatrix} 0 & 1 & 0 & 0 \\ 0 & 0 & 0 & -1 \\ 1 & 0 & 0 & 0 \\ 0 & 0 & 1 & 0 \end{bmatrix} \in \mathrm{SO}(4,\mathbb{R}) \quad , \tag{10}$$

see also table 3 in [19].

Now we carry out the analogous considerations for the manifold $N3$.

Face gluings N3: Opposite faces of the cube are glued,

$$N3: \; F1 \cup F6, \; F2 \cup F4, \; F3 \cup F5. \tag{11}$$

Edge gluing scheme N3: Directed edges in a single line are glued.

$$N3: \begin{bmatrix} 1 & 8 & 11 \\ 2 & \overline{6} & \overline{9} \\ 3 & 4 & \overline{12} \\ 5 & \overline{7} & \overline{10} \end{bmatrix} \tag{12}$$

Group $H = \mathrm{deck}(N3)$: The group $H = \mathrm{deck}(N3)$ is the binary dihedral group D_8^* generated by the two elements

$$\begin{gathered} g_1 := (g_{l1}, e) \;, \;\; g_2 := (g_{l2}, e) \\ \text{with } g_{l1} = \begin{bmatrix} 0 & \mathrm{i} \\ \mathrm{i} & 0 \end{bmatrix}, \; g_{l2} = \begin{bmatrix} \mathrm{i} & 0 \\ 0 & -\mathrm{i} \end{bmatrix}, \; e = \begin{bmatrix} 1 & 0 \\ 0 & 1 \end{bmatrix} \;, \end{gathered} \tag{13}$$

or equivalently by

$$R_{g_1} = \begin{bmatrix} 0 & -1 & 0 & 0 \\ 1 & 0 & 0 & 0 \\ 0 & 0 & 0 & -1 \\ 0 & 0 & 1 & 0 \end{bmatrix}, \; R_{g_2} = \begin{bmatrix} 0 & 0 & 0 & -1 \\ 0 & 0 & -1 & 0 \\ 0 & 1 & 0 & 0 \\ 1 & 0 & 0 & 0 \end{bmatrix} \in \mathrm{SO}(4, \mathbb{R}) \;. \tag{14}$$

2.2. Transformation of the observer position

Let us now address the question how the group $g \in H$ transforms under a change of the observer position, whereby each observer naturally puts his position at the origin of his coordinate system. The behaviour under such transformations will determine whether a spherical manifold is homogeneous or inhomogeneous. By applying an arbitrary transformation q to the coordinates

$$u \to u' = u\, q \;\; , \;\; q \in \mathrm{SU}(2, \mathbb{C}) \;\; , \tag{15}$$

we can transform the origin of the coordinate system to every point on $\mathbb{S}^3$ with the isometry q. By the transformation q, an observer sitting at $u = q^{-1}$ is shifted to the centre of the new coordinate system $u' = e$. Now consider a given point whose coordinates with respect to two observers o and o' are related by $u' = uq$. The group elements of the deck transformation with respect to the observer o is given by $g_i = (g_{li}, g_{ri})$, $i = 1, 2, \ldots$. Using these deck transformations we get for every point u

on the 3-sphere points $\tilde{u}_i$ that are to be identified, i. e. $\tilde{u}_i \equiv (g_{li})^{-1}\, u\, g_{ri}$. Transforming these points into the observer system o' we get

$$\begin{aligned} \tilde{u}_i \rightarrow \tilde{u}'_i = \tilde{u}_i\, q &= (g_{li})^{-1}\, u\, g_{ri}\, q \\ &= (g_{li})^{-1}\, u\, q\, (q^{-1}\, g_{ri}\, q) = (g_{li})^{-1}\, u'\, (q^{-1}\, g_{ri}\, q) \quad . \end{aligned} \tag{16}$$

The observer o' uses the equation $\tilde{u}'_i = (g'_{li})^{-1}\, u'\, g'_{ri}$ to identify points on the 3-sphere. Comparing this equation with eq. (16), one gets the deck transformations

$$g'_i \;=\; (g'_{li}, g'_{ri}) \;=\; (g_{li}, q^{-1}\, g_{ri}\, q) \quad , \quad i = 1, 2, \ldots \quad , \tag{17}$$

with respect to the observer o'. Since the coordinate transformation q is given by right action, the left action g_{li} of a deck transformation g_i does not change, but the right action g_{ri} of a deck transformation g_i in general changes under a coordinate transformation q.

In case of the manifold $N3$, the group elements $g_i = (g_{li}, e) = g'_i$, $i = 1, ..., 8$, see eq. (13), do not change under the transformation (15) because of $g_{ri} = e$. The invariance of the group elements implies that the same fundamental domain is obtained for every choice of the coordinate system. Such manifolds are called homogeneous, see e. g. p. 230 in [43]. In the case of the manifold $N2$ the transformation (15) changes the corresponding group elements $g_i = (g_{li}, g_{ri}) \rightarrow g'_i = (g_{li}, g'_{ri}) = (g_{li}, q^{-1}\, g_{ri}\, q)$, $i = 1, ..., 8$. Because of $q^{-1}\, g_{ri}\, q \neq g_{ri}$, in general, a different choice of the observer position usually result in another shape of the Voronoi domain, see eq. (1). Such a manifold is called an inhomogeneous manifold. These changes in the shape of the fundamental domain are illustrated in fig. 3, where the position of the observer is shifted using the parameterisation

$$q(\rho, \alpha, \epsilon) \;=\; \begin{bmatrix} \cos(\rho)\, \exp(-\mathrm{i}\alpha) & -\mathrm{i}\sin(\rho)\, \exp(-\mathrm{i}\epsilon) \\ -\mathrm{i}\sin(\rho)\, \exp(+\mathrm{i}\epsilon) & \cos(\rho)\, \exp(+\mathrm{i}\alpha) \end{bmatrix} \tag{18}$$

with $\rho \in [0, \frac{\pi}{2}]$, $\alpha, \epsilon \in [0, 2\pi]$.

2.3. Relation of the lens manifold $L(8,3)$ and $N2$.

To discuss the relation between these two spherical manifolds we look at their representations. With the generator $g = (g_l, g_r)$ of the group $H = C_8$ for the cubic manifold $N2$ given in eq. (6), it is easy to transform the generator g to diagonal form $g_d := (\delta_l, \delta_r)$,

$$\begin{aligned} \delta_l := g_l \;&=\; \begin{bmatrix} \overline{a} & 0 \\ 0 & a \end{bmatrix} \;=\; \begin{bmatrix} \exp(-\mathrm{i}\frac{\pi}{4}) & 0 \\ 0 & \exp(\mathrm{i}\frac{\pi}{4}) \end{bmatrix} , \\ \delta_r := q^{-1}\, g_r\, q \;&=\; q^{-1} \begin{bmatrix} 0 & a^3 \\ a & 0 \end{bmatrix} q \;=\; \begin{bmatrix} \exp(-\mathrm{i}\frac{\pi}{2}) & 0 \\ 0 & \exp(\mathrm{i}\frac{\pi}{2}) \end{bmatrix} , \end{aligned} \tag{19}$$

where the coordinate shift q, eq. (18), has to be chosen as

$$q \;=\; q\left(\rho = \frac{\pi}{4}, \alpha = \frac{7\pi}{8}, \epsilon = \frac{3\pi}{8}\right) \;=\; \frac{1}{\sqrt{2}} \begin{bmatrix} -\exp(\mathrm{i}\frac{\pi}{8}) & -\exp(\mathrm{i}\frac{\pi}{8}) \\ \exp(-\mathrm{i}\frac{\pi}{8}) & -\exp(-\mathrm{i}\frac{\pi}{8}) \end{bmatrix} . \tag{20}$$

If we define a transformation of coordinates u according to

$$u \to u' = \begin{bmatrix} x'_0 - \mathrm{i}x'_3 & -x'_2 - \mathrm{i}x'_1 \\ x'_2 - \mathrm{i}x'_1 & x'_0 + \mathrm{i}x'_3 \end{bmatrix} = u\,q \quad , \tag{21}$$

the action of the generator $g_d = (\delta_l, \delta_r)$ on the new coordinates u' follows from eq. (17)

$$u' \to \delta_l^{-1} u' \delta_r \quad . \tag{22}$$

This action can be expressed in terms of the complex coordinates (z'_1, z'_2) of u' by

$$g_d : (z'_1, z'_2) \to (z'_1\,\overline{a},\ z'_2\,a^3) \ = \ \left(z'_1 \exp\left(\mathrm{i}\frac{-2\pi}{8}\right),\ z'_2 \exp\left(\mathrm{i}\frac{3\cdot 2\pi}{8}\right)\right) \tag{23}$$

with $a = \exp(2\pi\mathrm{i}/8)$. Using the parameterisation (18) also for the coordinate u, the action of the generator $g_d = (\delta_l, \delta_r)$ is given by

$$g_d : u(\rho, \alpha, \epsilon) \to u\left(\rho, \alpha + \frac{2\pi}{8}, \epsilon - \frac{3\cdot 2\pi}{8}\right) \quad . \tag{24}$$

The complex representation (22) of the cubic generator g_d of the manifold $N2$ corresponds in the (real) classification by representations of Wolf [43] p. 224 exactly to the spherical lens space $L(n,k) = L(8,3)$. From this algebraic equivalence of the representations of C_8 for the lens manifold $L(8,3)$ according to [43] and for the cubic manifold $N2$, eq. (22), we conclude that there must exist a one-to-one geometric map of their fundamental domains. Their homotopy and deck group H must coincide.

In the following, we choose for the generator of the cyclic group C_8 the equivalent diagonalised generator $g = (\tilde{\delta}_l, \tilde{\delta}_r) := (\overline{\delta}_r, \overline{\delta}_l)$ that is

$$\tilde{\delta}_l = \begin{bmatrix} \exp(\mathrm{i}\frac{\pi}{2}) & 0 \\ 0 & \exp(-\mathrm{i}\frac{\pi}{2}) \end{bmatrix} \quad , \quad \tilde{\delta}_r = \begin{bmatrix} \exp(\mathrm{i}\frac{\pi}{4}) & 0 \\ 0 & \exp(-\mathrm{i}\frac{\pi}{4}) \end{bmatrix} \quad . \tag{25}$$

This generator and the generator $g_d := (\delta_l, \delta_r)$ describe isospectral manifolds. In [14] the following Theorem is proven: "If two 3-dimensional spherical space forms are isospectral, then they are isometric." Thus, the two generators lead to equivalent manifolds.

The action of the generator $g = (\tilde{\delta}_l, \tilde{\delta}_r)$, eq. (25), changes the negative sense of the rotation in the x_1-x_2-plane described in eq.(24) into a positive sense

$$g : u(\rho, \alpha, \epsilon) \to u\left(\rho, \alpha + \frac{2\pi}{8}, \epsilon + \frac{3\cdot 2\pi}{8}\right) \quad . \tag{26}$$

The Voronoi domain of the group generated by (26) is pictured in fig. 3a. The Voronoi domain is shown as a projection onto $\mathbb{R}^3$. This projection is defined as simply omitting the component x_0 in the vector $\vec{x}$, see eq. (9). The Voronoi cell is computed with respect to an observer at the origin $\vec{x}_0 = (1,0,0,0)$ by transforming the group elements of $L(8,3)$ using eq. (17). Now choosing in eq. (18) for the parameters $\alpha, \epsilon = 0$, we obtain for $\rho = 0.08\pi,\ 0.15\pi$, and 0.25π new generators $g' = (\tilde{\delta}_l, q^{-1}\tilde{\delta}_r q)$. The outcome of these are the Voronoi domains shown in figures 3b-d. For three values of ρ the actions of the deck transformations result in fundamental cells with very special shapes. For $\rho = 0$ the Voronoi domain is given by a spherical lens and for $\rho = 0.25\pi$ by the spherical Platonic

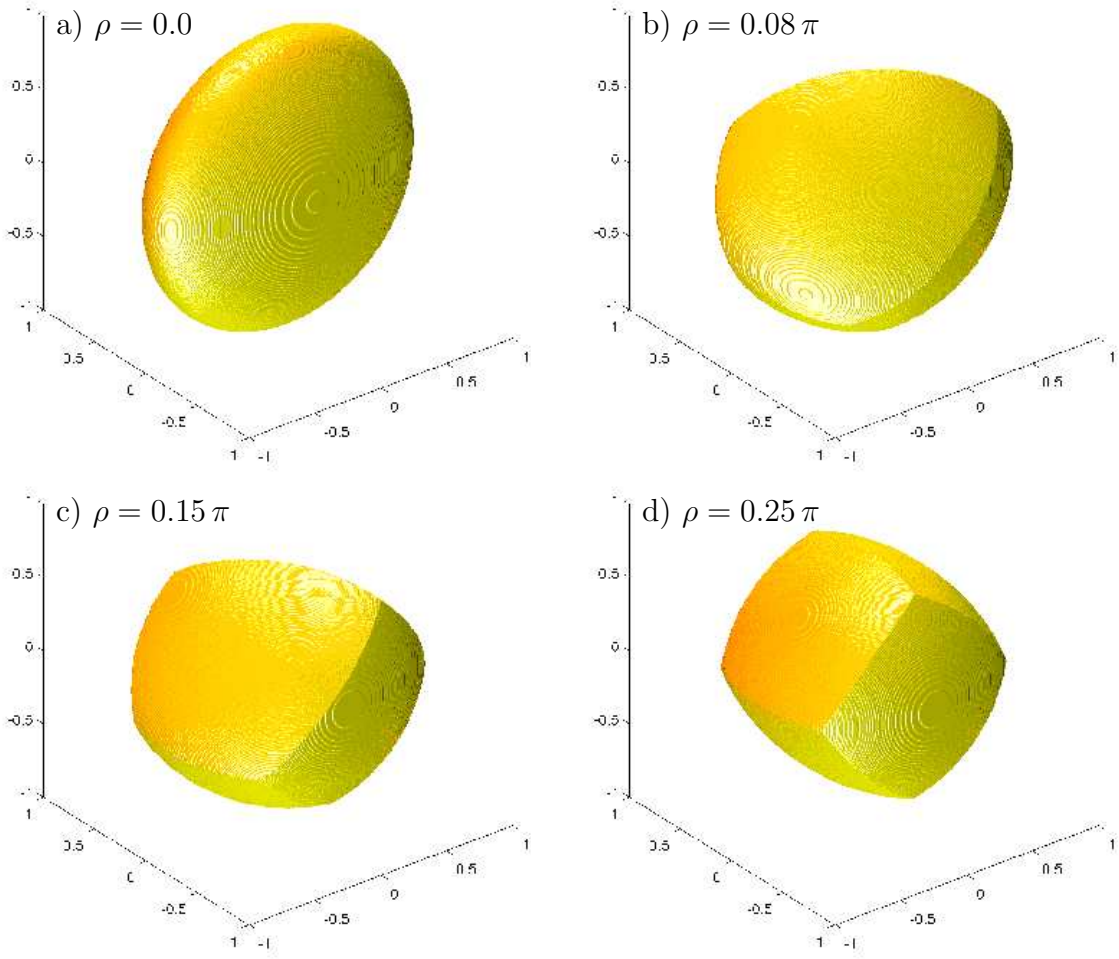

Figure 3. The Voronoi domains of the manifold $L(8,3) \equiv N2$ at four different positions of the observer q^{-1} are shown using the projection to $\mathbb{R}^3$. Within the parameterisation of the observer point, see eq. (18), the coordinate ρ is varied. In doing so $\alpha, \epsilon = 0$ have been chosen.

cube $N2$, as revealed by eq. (20) using $\sin\frac{\pi}{4} = \cos\frac{\pi}{4} = \frac{1}{\sqrt{2}}$. In the case of $\rho = 0.5\pi$ the generator of the group transforms to $g' = (\tilde{\delta}_l, \tilde{\overline{\delta}}_r) = (\overline{\delta}_r, \delta_l)$ again resulting in the geometric shape of a spherical lens, but the action of this generator on the coordinate u' have been exchanged compared to eq. (26), $g' : u'(\rho, \alpha, \epsilon) \to u'(\rho, \alpha + \frac{3\cdot 2\pi}{8}, \epsilon + \frac{2\pi}{8})$.

2.4. The lens manifold $L(8,1)$.

In addition to $L(8,3) \equiv N2$ there is another specification of the abstract group C_8 which results in the lens space $L(8,1)$. The generator of this group can be chosen as

$$g := (g_l, e) \quad \text{with} \quad g_l := \begin{bmatrix} \exp\left(\mathrm{i}\frac{\pi}{4}\right) & 0 \\ 0 & \exp\left(-\mathrm{i}\frac{\pi}{4}\right) \end{bmatrix} \quad . \tag{27}$$

The action of the generator (27) on the coordinate u is given by

$$g : u(\rho, \alpha, \epsilon) \to u\left(\rho, \alpha + \frac{2\pi}{8}, \epsilon + \frac{2\pi}{8}\right) \quad . \tag{28}$$

This realisation of the cyclic group C_8 describes a homogeneous manifold. The Voronoi domain of this manifold is a spherical lens similar to the case $\rho = 0.0$ of the manifold $L(8,3)$. But the actions of these two cyclic groups C_8 are not equivalent as the comparison of (28) with (26) shows.

3. Eigenmodes of spherical manifolds and sums related to them.

3.1. Harmonic analysis on a spherical manifold.

From deck groups acting on the 3-sphere $\mathbb{S}^3$ one can go globally to harmonic analysis on the 3-sphere. One can establish functional analysis globally on the cover by determining a complete set of functions on the 3-sphere, each of them invariant under the action of the chosen group $H = \mathrm{deck}(\mathcal{M})$. The same set of functions, restricted to the prototile $\mathcal{M}$, locally obeys its homotopic boundary conditions and so yields a local basis on it.

Since the group H is a subgroup of $\mathrm{SO}(4,\mathbb{R})$, it also commutes with the Euclidean Laplacian Δ on $\mathbb{E}^4$. By restricting the set of functions to those that vanish under Δ, termed harmonic, we are doing harmonic analysis on the manifold $\mathcal{M}$.

For all spherical manifolds, the global covering 3-sphere $\mathbb{S}^3$ and its eigenmodes form an arena of comparison. By extending any H-invariant polynomial to a polynomial function on the 3-sphere, we circumvent the need to explicitly identify any point or functional value on the sphere with a point or functional value on the chosen single topological manifold $\mathcal{M}$. The Wigner polynomials $D^j_{m_1,m_2}(u)$, $u \in \mathrm{SU}(2,\mathbb{C})$, introduced by Wigner [42] for the analysis on $\mathrm{SU}(2,\mathbb{C})$, for all degrees $2j = 0, 1, 2, ..., \infty$ form an orthogonal and complete set of harmonic functions on the 3-sphere $\mathbb{S}^3$ [21]. The general action of $\mathrm{SO}(4,\mathbb{R}) \sim (\mathrm{SU}^l(2,\mathbb{C}) \times \mathrm{SU}^r(2,\mathbb{C}))/\{\pm(e,e)\}$ with elements $g = (g_l, g_r)$ on Wigner polynomials and its representation from eqs. (4) and (5) are

$$\begin{aligned}(T_{(g_l,g_r)} D^j_{m_1 m_2})(u) &:= D^j_{m_1 m_2}(g_l^{-1} u g_r) \\ &= \sum_{m_1' m_2'} D^j_{m_1' m_2'}(u)\, D^j_{m_1 m_1'}(g_l^{-1})\, D^j_{m_2' m_2}(g_r). \end{aligned} \tag{29}$$

Therefore, we can write the basis of the harmonic analysis on $\mathcal{M}$ to its H-invariant subbasis by projection from Wigner polynomials.

We introduce the Wigner basis, compare [21], with $\beta = 2j + 1$,

$$\psi(j, m_1, m_2)(u) \;=\; \frac{2j+1}{\sqrt{2\,\pi^2}}\, \langle j - m_1 j m_1 | 00 \rangle\; D^j_{-m_1 m_2}(u) \quad , \tag{30}$$

which is normalised on the 3-sphere $\mathbb{S}^3$. In the following, we use the spherical basis

$$\psi(j, l, m)(u) \;=\; \sum_{m_1} \psi(j, m_1, m_2)(u)\; \langle j m_1 j m_2 | l m \rangle \tag{31}$$

which is related to the Wigner basis also by

$$\psi(j, m_1, m_2)(u) \;=\; \sum_{l} \psi(j, l, m)(u)\; \langle j m_1 j m_2 | l m \rangle \quad , \tag{32}$$

where $\langle jm_1jm_2|lm\rangle$ are the Clebsch-Gordan coefficients which obey $0 \leq l \leq 2j$ and $m = m_1 + m_2$. More details on these coefficients are given e. g. in [8]. The spherical basis eq. (31) has the property that under the conjugation action of $\mathrm{SU}^c(2,\mathbb{C})$, it transforms as

$$h = (g,g) \ : (T_{g,g}\psi)(j,l,m)(u) = \psi(j,l,m)(g^{-1}ug) \\ = \sum_{m'} \psi(j,l,m')(u)\ D^l_{m'm}(R(g)) \ , \qquad (33)$$

where $R(g)$ is the rotation w.r.t. the coordinates (x_1, x_2, x_3) that corresponds to $g \in \mathrm{SU}^C(2,\mathbb{C})$. With a set (χ, θ, ϕ) of coordinates for u [2, 21], the spherical basis is proportional to the standard spherical harmonics $Y^l_m(\theta,\phi)$ and is given by $\psi(j,l,m)(\chi,\theta,\phi) = \mathrm{i}^l R^l_\beta(\chi) Y^l_m(\theta,\phi)$ with

$$R^l_\beta(\chi) = (-\mathrm{i})^l \sqrt{\frac{2\beta^2}{(2l+1)}} \sum_{m_1} \langle j - m_1 j m_1|00\rangle \langle j - m_1 j m_1|l0\rangle D^j_{m_1 m_1}(\chi,0,\chi) \quad ,$$

see [12]. A different phase convention for the radial function is used as in [12]. This spherical basis is very convenient for the multipole expansion of invariant polynomials.

What happens to the CMB multipole amplitudes when we adopt on the manifold a general position of the observer?

We use Cartesian coordinates x in Euclidean 4-space and 2×2 matrix coordinates $u(x)$ and write down the general transformation $u \to u' = u\,q$, $x \to x' = x\,R(q)$ of the coordinates from a special point (for example the centre of a spherical space) to a general point.

Then we can pass to polynomial functions (Wigner or spherical) and give on the 3-sphere their transformation law as a function of $(q,\ R(q))$. We focus on the spherical basis and show how the multipole expansion in a given topological model is transformed under change of the observer position into another multipole expansion.

Our initial basis on the 3-sphere are linear combinations of Wigner polynomials in initial coordinates u, convenient for the initial observer or suggested by a simple decomposition under H. The most general shift of the observer to new coordinates u' is given by eq. (15). The unitary matrix transformation $u \to u' = u\,q$ yields a rotation $R(q) : x' = x\,R(q)$, applied to the row of coordinates $x = (x_0, x_1, x_2, x_3)$ of Euclidean space $\mathbb{E}^4$, given by

$$u = \begin{bmatrix} z_1 & z_2 \\ -\overline{z}_2 & \overline{z}_1 \end{bmatrix} = \begin{bmatrix} x_0 - \mathrm{i}x_3 & -x_2 - \mathrm{i}x_1 \\ x_2 - \mathrm{i}x_1 & x_0 + \mathrm{i}x_3 \end{bmatrix},\ q = \begin{bmatrix} a & b \\ -\overline{b} & \overline{a} \end{bmatrix}, \qquad (34)$$

$$R(q) = \frac{1}{2} \begin{bmatrix} (a+\overline{a}) & \mathrm{i}(b-\overline{b}) & -(b+\overline{b}) & \mathrm{i}(a-\overline{a}) \\ -\mathrm{i}(b-\overline{b}) & -(a+\overline{a}) & \mathrm{i}(a-\overline{a}) & -(b+\overline{b}) \\ (b+\overline{b}) & -\mathrm{i}(a-\overline{a}) & -(a+\overline{a}) & -\mathrm{i}(b-\overline{b}) \\ -\mathrm{i}(a-\overline{a}) & (b+\overline{b}) & \mathrm{i}(b-\overline{b}) & (a+\overline{a}) \end{bmatrix}.$$

3.2. Observer- and multipole dependence in the spherical basis.

Initially, the coordinates on the 3-sphere refer to the point $(1,0,0,0)$, $u = e$. We now pass with eq. (34) to a general position of the observer.

Our approach to the dependence of the multipole analysis on the observer position goes as follows: We break the general right transformation (e, q) of the coordinates into a diagonal part λ and two rotations from $\mathrm{SO}(3,\mathbb{R})$. We use the bracket notation. The matrix $q \in \mathrm{SU}(2,\mathbb{C})$ has a diagonal decomposition

$$q = r\lambda r^{-1} \ . \tag{35}$$

Now for elements $(g_l, g_r) \in \mathrm{SO}(4,\mathbb{R}) \sim (\mathrm{SU}^l(2,\mathbb{C}) \times \mathrm{SU}^r(2,\mathbb{C}))/(\pm(e,e))$, we have the identity

$$(r,r)(e,\lambda)(r^{-1},r^{-1}) = (e, r\lambda r^{-1}) = (e,q) \ . \tag{36}$$

We consider the three factors on the left hand side and compute their matrix elements in the representation of $\mathrm{SO}(4,\mathbb{R})$.

(i) In the spherical basis $\psi(j,l,m)(u), \beta = 2j+1$, we have

$$\langle jlm|T_{(r,r)}|jl'm'\rangle = \delta_{ll'} D^l_{mm'}(R(r)), \tag{37}$$

where $R(r)$ is the rotation from $\mathrm{SO}(3,\mathbb{R})$ acting on (x_1,x_2,x_3) that corresponds to $r \in \mathrm{SU}(2,\mathbb{C})$.

(ii) In the Wigner polynomial basis $D^j_{m_1,m_2}(u)$ we have for the diagonal part

$$\lambda = \begin{bmatrix} \exp(\mathrm{i}\alpha/2) & 0 \\ 0 & \exp(-\mathrm{i}\alpha/2) \end{bmatrix} \ , \ \cos(\alpha/2) = \mathrm{Trace}(q)/2 \ , \tag{38}$$
$$\langle jm_1m_2|T_{(e,\lambda)}|jm_1'm_2'\rangle = \delta_{m_1m_1'}\delta_{m_2m_2'} \exp(\mathrm{i}\alpha(m_1-m_2)) \ .$$

The diagonal part λ is completely determined by the trace. Transforming these matrix elements into the spherical basis eq. (31) gives with eq. (38)

$$\begin{aligned} &\langle jlm|T_{(e,\lambda)}|jl'm'\rangle \\ &\quad = \sum_{m_1m_2} \langle lm|j-m_1jm_2\rangle \exp(\mathrm{i}\alpha(m_1-m_2))\langle j-m_1jm_2|l'm'\rangle \ . \end{aligned} \tag{39}$$

where two sign factors cancel. Now we combine the three factors from eq. (36) to obtain the overall matrix elements in the spherical basis as

$$\begin{aligned} &\langle jlm|T_{(e,q)}|jl'm'\rangle \\ &\quad = \sum_{m''} D^l_{mm'}(R(r))\langle jlm'|T_{(e,\lambda)}|jl'm''\rangle D^{l'}_{m''m'}(R^{-1}(r)) \end{aligned} \tag{40}$$

with the middle matrix elements given in eq. (39). The matrix elements in the middle are the essential part of the transformation to a new observer position. Under the rotations $R(r), R(r^{-1})$, the bases in multipole form have standard properties.

Proposition: The spherical basis under transformation of the observer position eq. (34) transforms according to eq. (40).

3.3. Application to the spherical manifolds $N2 \equiv L(8,3)$, $L(8,1)$, and $N3$.

Using eq. (25) it is easy to construct the set of polynomials $\psi(j,m_1,m_2)(u)$, see eq. (30), which form the basis of harmonic analysis on the manifold $N2$: To have a Wigner polynomial

$$D^j_{-m_1,m_2}(u) = \exp\left[-\mathrm{i}\,(\alpha+\epsilon)\,m_1\right] d^j_{-m_1,m_2}(2\rho) \exp\left[\mathrm{i}\,(\alpha-\epsilon)\,m_2\right] \tag{41}$$

in the coordinates $u = u(\rho,\alpha,\epsilon)$ invariant under the action of the generator (26) of $H = C_8$ requires

$$\psi^{N2}(j,m_1,m_2)(u) \;=\; \psi(j,m_1,m_2)(u) :\; 2\,m_1 + \,m_2 \equiv 0 \bmod 4 \quad . \tag{42}$$

In a (m_1,m_2)-lattice on the plane (see fig. 5 in [22]), we can choose the sublattice with lattice basis vectors

$$\vec{a}_1 = (-1,2) \quad , \quad \vec{a}_2 = (1,2) \quad . \tag{43}$$

Then any sublattice point obeys eq. (42), and the harmonic basis for $N2$ consists of the towers of polynomials $\psi(j,m_1,m_2)(u)$ over this sublattice point with $j = j_0 + \nu, \nu = 0,1,2,,..,j_0 = \mathrm{Max}(|m_1|,|m_2|)$. In general, similar eigenmodes on the lens spaces are reported in [25] and equivalent sets of eigenmodes on the lens spaces in [26, 27].

On the lens space $L(8,1)$, the action of the generator (28) leads to the eigenmodes in the Wigner basis

$$\psi^{L(8,1)}(j,m_1,m_2)(u) \;=\; \psi(j,m_1,m_2)(u) :\; m_1 \equiv 0 \bmod 4 \quad . \tag{44}$$

The invariant eigenfunctions of the Laplace-Beltrami operator on $N3$ in the Wigner basis are determined by (13) as

$$\begin{aligned} &\psi^{N3}(j,m_1,m_2)(u) \qquad\qquad\qquad\qquad\qquad\qquad\qquad\qquad (45)\\ &= \begin{cases} \frac{1}{\sqrt{2}}\left(\psi(j,m_1,m_2)(u) + (-1)^{m_1}\,\psi(j,-m_1,m_2)(u)\right) & : \; j \text{ even}, m_1 > 0 \\ \psi(j,m_1,m_2)(u) & : \; j \text{ even}, m_1 = 0 \\ \frac{1}{\sqrt{2}}\left(\psi(j,m_1,m_2)(u) - (-1)^{m_1}\,\psi(j,-m_1,m_2)(u)\right) & : \; j \text{ odd}, m_1 > 0 \end{cases} \end{aligned}$$

where $j \in \{0,2,3,4,...\}$, $m_2 \in \mathbb{Z}$, $m_1 \in \mathbb{N}_0$, $m_1 \equiv 0 \bmod 2$, and $m_1, |m_2| \leq j$. A similar result is stated in [25] and an equivalent set of the eigenmodes in [26, 27].

Under the transformation (15) to arbitrary new coordinates, the relation $\psi'^{N3}(j,m_1,m_2)(\tilde{u}') \;=\; \psi^{N3}(j,m_1,m_2)(\tilde{u})$ holds, because the eigenfunctions of the Laplace-Beltrami operator are scalar functions. For this reason we get in the case of $N3$ for $\tilde{u} = uq^{-1}$

$$\begin{aligned} \psi'^{N3}(j,m_1,m_2)(u) &= \psi^{N3}(j,m_1,m_2)(u\,q^{-1}) \\ &= \sum_{\tilde{m}_2=-j}^{j} \psi^{N3}(j,m_1,\tilde{m}_2)(u)\, D^j_{\tilde{m}_2,m_2}(q^{-1}) \end{aligned} \tag{46}$$

for all allowed values of m_1 and m_2. In general such an expansion is possible for all eigenfunctions on homogeneous spherical manifolds using the Wigner basis. Since for

every $|m_2| \leq j$ an eigenfunction on $N3$ exists we can choose a new equivalent basis of eigenfunctions in the coordinates u which is given by

$$\begin{aligned}\tilde{\psi}'^{N3}(j,m_1,m_2)(u) &= \sum_{\tilde{m}_2=-j}^{j} \psi'^{N3}(j,m_1,\tilde{m}_2)(u)\, D^j_{\tilde{m}_2,m_2}(q) \\ &= \sum_{\tilde{m}_2=-j}^{j} \psi^{N3}(j,m_1,\tilde{m}_2)(u\,q^{-1})\, D^j_{\tilde{m}_2,m_2}(q) \\ &= \psi^{N3}(j,m_1,m_2)(u) \quad . \end{aligned} \tag{47}$$

Here the transformation (46) and $\sum_{\tilde{m}_2=-j}^{j} D^j_{m_1,\tilde{m}_2}(q^{-1})\, D^j_{\tilde{m}_2,m_2}(q) = \delta_{m_1,m_2}$ are used. The last step requires that there are no restrictions on m_2. A restriction on m_2 would lead to observer dependent eigenfunctions. The above calculation shows that we can choose for all coordinate shifts q^{-1} of the observer the same basis of eigenfunctions. For this reason the CMB properties do not depend on the position of the observer in a homogeneous manifold.

In the case of the eigenfunctions (42) on the other manifold $N2$, not all values of $|m_2| \leq j$ are allowed. For this reason we cannot make an analog choice of the eigenfunctions as on $N3$, and hence the analysis on $N2$ shows a dependence of the observer. Expanding the eigenfunctions (42) on $N2$ with respect to the basis (30) we get

$$\begin{aligned}\psi'^{N2}(j,m_1,m_2)(u) &= \psi^{N2}(j,m_1,m_2)(u\,q^{-1}) \\ &= \sum_{\tilde{m}_2=-j}^{j} \psi(j,m_1,\tilde{m}_2)(u)\, D^j_{\tilde{m}_2,m_2}(q^{-1}) \end{aligned} \tag{48}$$

with the restriction $2\,m_1 + m_2 \equiv 0 \mod 4$. This restriction on m_2 prohibits a new basis analogous to (47). Here q^{-1} gives the position of the observer with respect to the coordinate system where the Voronoi domain is given as a spherical lens, see fig. 3.

Using eq. (31) we can transform the eigenfunctions into an expansion with respect to the spherical basis $\psi(jlm)(u)$:

$$\begin{aligned}\psi'^{N2}(j,m_1,m_2)(u) &= \sum_{l=0}^{2j} \sum_{m=-l}^{l} \xi^{j,\rho(m_1,m_2)}_{lm}(N2;q)\, \psi(j,l,m)(u) \quad , \\ \xi^{j,\rho(m_1,m_2)}_{lm}(N2,q) &= \langle j m_1 j \tilde{m}_2 | lm \rangle\, D^j_{\tilde{m}_2,m_2}(q^{-1}) \end{aligned} \tag{49}$$

where $2\,m_1 + m_2 \equiv 0 \mod 4$, $m_1 + \tilde{m}_2 = m$, and $1 \leq \rho(m_1,m_2) \leq r^{N2}(\beta)$ counts the multiplicity $r^{N2}(\beta)$ of the eigenvalue E_j of the Laplace-Beltrami operator on $N2$ for $j \in \mathbb{N}_0$. The multiplicity for $1 \leq j \leq 4$ is given in table 1. The expansion (49) is convenient for the following applications.

On the homogeneous manifold $N3$ we can get a similar expansion of the eigenfunctions

$$\psi'^{N3}(j,m_1,m_2)(u) = \sum_{l=0}^{2j} \sum_{m=-l}^{l} \xi^{j,\rho(m_1,m_2)}_{lm}(N3)\, \psi(j,l,m)(u)$$

$$\xi_{lm}^{j,\rho(m_1,m_2)}(N3) \tag{50}$$
$$= \begin{cases} \frac{1}{\sqrt{2}}\left(\langle jm_1jm_2|lm\rangle + \langle j-m_1jm_2|lm\rangle\right) & : \; j \text{ even}, m_1 > 0 \\ \langle j0jm_2|lm\rangle & : \; j \text{ even}, m_1 = 0 \\ \frac{1}{\sqrt{2}}\left(\langle j-m_1jm_2|lm\rangle - \langle jm_1jm_2|lm\rangle\right) & : \; j \text{ odd}, m_1 > 0 \end{cases}$$

where $m_1 \equiv 0 \mod 2$, $0 \leq m_1 \leq j$, $|m_2| \leq j$, and $j \in \{0, 2, 3, 4, ...\}$. As shown above we can choose the same expansion for all positions of the observer in this case. The calculation of the ensemble average of the angular power spectrum (56) or the 2-point correlation function (54) requires the evaluation of the following sums. For the homogeneous $N3$ space, using eq. (3.5.15) in [8], one obtains

$$\begin{aligned} &\frac{1}{2l+1}\sum_{m=-l}^{l}\sum_{m_1}\sum_{m_2=-j}^{j}\left|\xi_{lm}^{j,\rho(m_1,m_2)}(N3)\right|^2 \\ &\quad = \frac{1}{2l+1}\sum_{m=-l}^{l}\sum_{m_1}\sum_{m_2=-j}^{j}\langle jm_1jm_2|lm\rangle^2 \\ &\quad = \frac{1}{2j+1}\sum_{m=-l}^{l}\sum_{m_1}\sum_{m_2=-j}^{j}\langle j-m_2lm|jm_1\rangle^2 \\ &\quad = \frac{1}{2j+1}\sum_{m_1}1 \;=\; \frac{r^{N3}(\beta)}{\beta^2} \quad , \end{aligned} \tag{51}$$

and for the inhomogeneous $N2$ space with its restrictions on m_2 ($2m_1 + m_2 = 0 \mod 4$)

$$\begin{aligned} &\frac{1}{2l+1}\sum_{m=-l}^{l}\sum_{m_1,m_2}\left|\xi_{lm}^{j,\rho(m_1,m_2)}(N2;q)\right|^2 \\ &\quad = \frac{1}{2l+1}\sum_{m=-l}^{l}\sum_{m_1,m_2}\left|\langle jm_1j\tilde{m}_2|lm\rangle\, D^j_{\tilde{m}_2,m_2}(q^{-1})\right|^2 \\ &\quad = \frac{1}{2l+1}\sum_{m=-l}^{l}\sum_{m_1,m_2}\left|\langle jm_1j\tilde{m}_2|lm\rangle\, d^j_{\tilde{m}_2,m_2}(-2\rho)\right|^2 \quad . \end{aligned} \tag{52}$$

In the derivation of eq. (52) we have used eq. (41) where the coordinates of the observer position on the manifold are parameterised by eq. (18). The d-functions are computed using the algorithm described in [32]. The important point is that eq. (51) is independent of the observer position, whereas eq. (52) has an explicit ρ dependence. Eq. (51) applies on all homogeneous spherical manifolds $\mathcal{M}$ using the corresponding multiplicity $r^{\mathcal{M}}(\beta)$ of the eigenmodes [1, 12, 2, 4, 30]. Thus this equation is also true for the manifold $L(8,1)$.

The following transformation shows that the observers at ρ and at $\pi/2 - \rho$ see the same CMB anisotropies in the statistical sense. Substituting in eq. (52) -2ρ by $\pi + 2\rho$ one gets

$$\frac{1}{2l+1}\sum_{m=-l}^{l}\sum_{m_1,m_2'}\left|\langle jm_1j\tilde{m}_2|lm\rangle\, d^j_{\tilde{m}_2,m_2'}(\pi+2\rho)\right|^2$$

$\beta = 2j+1$	$r^{L(8,1)}(\beta)$	$r^{N2}(\beta)$	$r^{N3}(\beta)$	$r^{\mathbb{S}^3}(\beta)/8$
3	3	1	0	1.125
4	0	0	0	2
5	5	7	10	3.125
6	0	0	0	4.5
7	7	11	7	6.125
8	0	0	0	8
9	27	23	27	10.125

Table 1. The multiplicity $r^{\mathcal{M}}(\beta)$ of the eigenmodes for the wave numbers β from 3 to 9 on the manifolds $\mathcal{M} = L(8,1)$, $N2 \equiv L(8,3)$, and $N3$ is specified. In the case of the 3-sphere the effective multiplicity is given which is the multiplicity $r^{\mathbb{S}^3}(\beta) = \beta^2$ divided by the order of the group $N_{L(8,1)} = N_{N2} = N_{N3} = 8$. Analytical formulae for the multiplicity of the eigenmodes are known for homogeneous spherical manifolds [15, 40] and for a specific class of the inhomogeneous spherical manifolds [30] but not for the manifold $N2$.

$$
\begin{aligned}
&= \frac{1}{2l+1} \sum_{m=-l}^{l} \sum_{m_1,m_2'} \left| \langle j m_1 j \tilde{m}_2 | l m \rangle \ (-1)^{(j-\tilde{m}_2)} \ d^j_{-\tilde{m}_2,m_2'}(-2\rho) \right|^2 \\
&= \frac{1}{2l+1} \sum_{m=-l}^{l} \sum_{m_1,m_2} \left| \langle j m_1 j - \tilde{m}_2 | l m \rangle \, d^j_{\tilde{m}_2,m_2}(-2\rho) \right|^2 \\
&= \frac{1}{2l+1} \sum_{m=-l}^{l} \sum_{m_1,m_2} \left| \langle j - m_1 j \tilde{m}_2 | l - m \rangle \, d^j_{\tilde{m}_2,m_2}(-2\rho) \right|^2 \\
&= \frac{1}{2l+1} \sum_{m=-l}^{l} \sum_{m_1,m_2} \left| \langle j m_1 j \tilde{m}_2 | l m \rangle \, d^j_{\tilde{m}_2,m_2}(-2\rho) \right|^2 \qquad (53)
\end{aligned}
$$

where eqs. (3.5.17) and (4.2.4) in [8] are used and that there exists to every eigenfunction with the numbers (m_1, m_2) also an eigenfunction with the numbers $(-m_1, m_2)$ on the manifold $N2$, see eq. (43). Thus, the CMB analysis of the space $N2$ can be restricted to the interval $\rho \in [0, \pi/4]$.

4. Observer dependence of the temperature 2-point correlation function of the CMB radiation.

The temperature correlations of the CMB sky with respect to their separation angle ϑ are an important diagnostic tool. The correlations at large angles ϑ, where the topological signature is expected, are most clearly revealed by the temperature 2-point correlation function $C(\vartheta)$ which is defined as

$$
C(\vartheta) \ := \ \langle \delta T(\hat{n}) \delta T(\hat{n}') \rangle \quad \text{with} \quad \hat{n} \cdot \hat{n}' = \cos\vartheta \quad , \qquad (54)
$$

where $\delta T(\hat{n})$ is the temperature fluctuation in the direction of the unit vector $\hat{n}$. The 2-point correlation function $C(\vartheta)$ is related to the multipole moments C_l by

$$C(\vartheta) \;=\; \sum_l \frac{2l+1}{4\pi}\, C_l\, P_l\left(\cos\vartheta\right) \quad . \tag{55}$$

The ensemble average of C_l can be expressed for a spherical manifold $\mathcal{M}$ by the expansion coefficients $\xi_{lm}^{\beta,\rho}(\mathcal{M};q)$ discussed in the previous section

$$\begin{aligned} C_l &:= \frac{1}{2l+1}\sum_{m=-l}^{l}\left\langle |a_{lm}|^2\right\rangle \\ &= \sum_\beta \frac{T_l^2(\beta)\; P(\beta)}{2l+1}\sum_{m=-l}^{l}\sum_\rho \left|\xi_{lm}^{\beta,\rho}(\mathcal{M};q)\right|^2 \quad , \end{aligned} \tag{56}$$

with the initial power spectrum $P(\beta)\sim 1/(E_\beta\,\beta^{2-n_s})$ where $E_\beta=\beta^2-1$ are the allowed eigenvalues of the Laplace-Beltrami operator on the considered spherical manifold $\mathcal{M}$, $\beta=2j+1$, and n_s is the spectral index. $T_l(k)$ is the transfer function containing the full Boltzmann physics, e. g. the ordinary and the integrated Sachs-Wolfe effect, the Doppler contribution, the Silk damping and the reionization are taken into account. Using the expression (52) for the expansion coefficients $\xi_{lm}^{\beta,\rho}(\mathcal{M};q)$ we get for the ensemble average of C_l on $N2$

$$C_l \;=\; \sum_\beta \frac{T_l^2(\beta)\; P(\beta)}{2l+1}\sum_{m=-l}^{l}\sum_{m_1,m_2}\left|\langle jm_1j\tilde{m}_2|lm\rangle\, d^j_{\tilde{m}_2,m_2}(-2\rho)\right|^2 \tag{57}$$

which depends only on the distance ρ. Therefore, also the ensemble average of the 2-point correlation function on $N2$ depends only on ρ. Since the sum over the expansion coefficient in eq. (57) fulfils the symmetry (53) the interval of ρ can be restricted to $\rho\in[0,\frac{\pi}{4}]$.

In contrast, using the sum rule (51), the ensemble average of C_l on $N3$ is given by

$$C_l \;=\; \sum_\beta T_l^2(\beta)\; P(\beta)\,\frac{r^{N3}(\beta)}{\beta^2} \tag{58}$$

which does not depend on the position of the observer. The multiplicity $r^{N3}(\beta)$ restricts the sum over β to $\beta\geq 5$ for $N3$. The relation (58) is valid for homogeneous manifolds. Thus, this equation also holds for the manifold $L(8,1)$ using the corresponding multiplicity of the eigenmodes on $L(8,1)$.

To speed up the calculations of the ensemble average of C_l on all three manifolds $\mathcal{M}$ = L(8,3)($\equiv N2$), $N3$ and $L(8,1)$ we have used for $\beta>50$ the spectrum of the projective space $\mathbb{P}^3$ divided by $V_\mathcal{M}/V_{\mathbb{P}^3}=4$. We have checked numerically that this is good approximation of the exact result. This approximation can be used in a similar way for all manifolds which tessellate the 3-sphere under a group of deck transformations of even order.

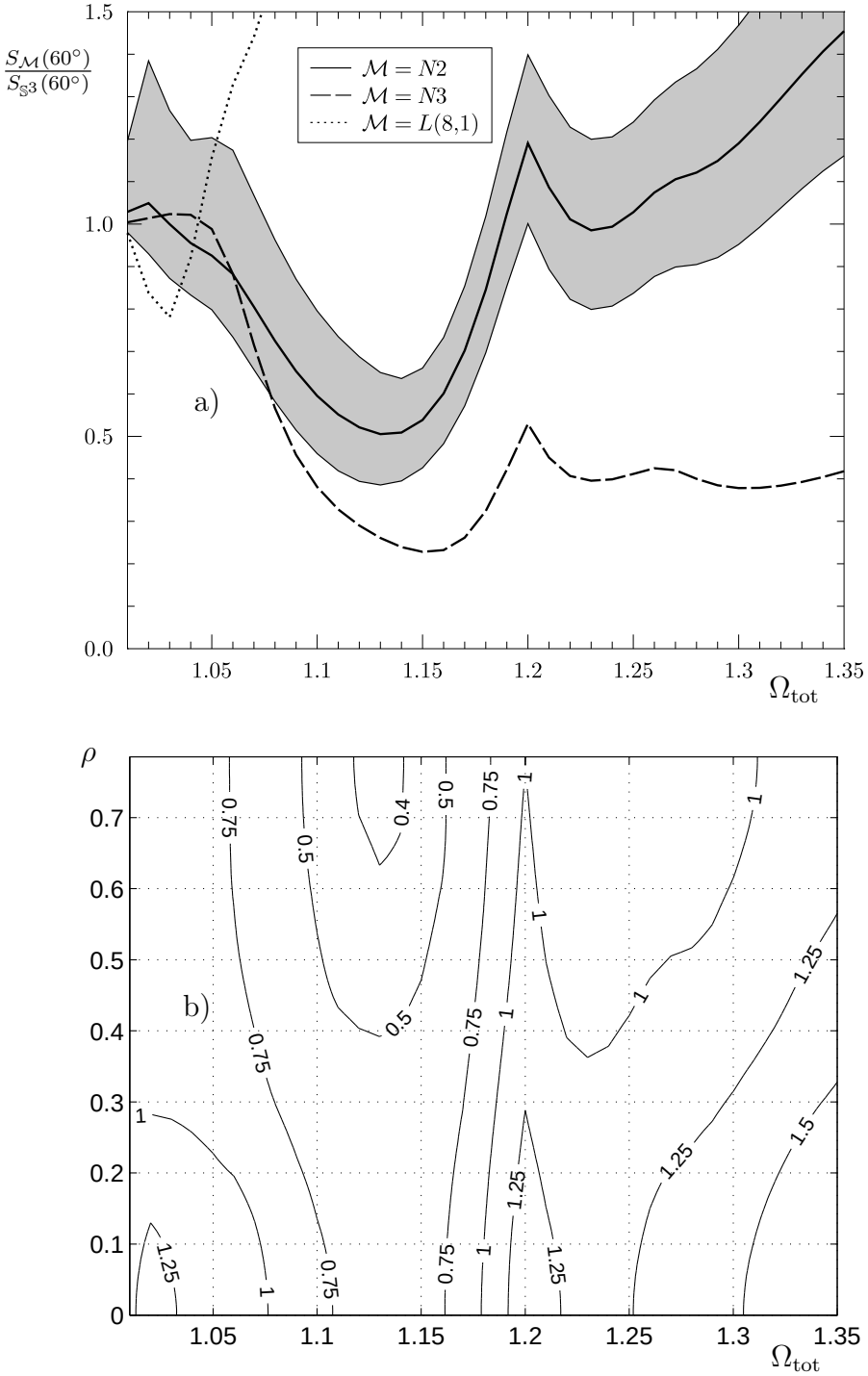

Figure 4. Panel a) shows the $S_{\mathcal{M}}(60°)$ statistics of the manifolds $\mathcal{M} = L(8,1)$, $L(8,3) \equiv N2$, and $N3$ normalised to the $S_{\mathbb{S}^3}(60°)$ statistics of the 3-sphere $\mathbb{S}^3$ depending on the total density parameter Ω_{tot}. In the case of the manifold $N2 \equiv L(8,3)$ the average of the $S_{L(8,3)}(60°)$ statistics due to the observer dependence is displayed as a full line. The dispersion of the $S_{L(8,3)}(60°)$ statistics depending on the observer is given by a grey band. In panel b) the $S_{L(8,3)}(60°)$ statistics normalised to the $S_{\mathbb{S}^3}(60°)$ statistics depending on Ω_{tot} and the observer position is displayed where the position of the observer is characterised by ρ.

The comparison of the various correlation functions $C(\vartheta)$ is facilitated by the introduction of the $S(60^\circ)$ statistics

$$S(60^\circ) := \int_{-1}^{\cos(60^\circ)} \mathrm{d}\cos\vartheta \, |C(\vartheta)| \quad . \tag{59}$$

It quantifies the power of the 2-point correlation function $C(\vartheta)$ on scales large than $\vartheta = 60^\circ$ which is the interesting scale for topological studies. This scalar quantity has been introduced in [38] in order to describe the low power at large angular scales which has been observed in the CMB sky.

In the following, the 2-point correlation functions are calculated for the cosmological parameters $\Omega_{\mathrm{cdm}} = 0.238$, $\Omega_{\mathrm{bar}} = 0.0485$, $h = 0.681$, and $n_{\mathrm{s}} = 0.961$. The density parameter of the cosmological constant Ω_Λ is changed according to get the desired total density parameter Ω_{tot}.

In fig. 4a the $S(60^\circ)$ statistics is presented for a wide range of the total density parameter Ω_{tot} for the three manifolds $L(8,1)$, $L(8,3) \equiv N2$, and $N3$. To emphasise the differences between the different topological spaces, the $S(60^\circ)$ statistics is normalised with respect to the simply-connected manifold $\mathbb{S}^3$, that is, the plot shows $\frac{S_{\mathcal{M}}(60^\circ)}{S_{\mathbb{S}^3}(60^\circ)}$. For these three manifolds the ensemble averages with respect to the sky realisations are shown. For the two homogeneous spaces $L(8,1)$ and $N3$ there is no observer dependence and thus, the result is shown as a dotted and dashed curve, respectively. The inhomogeneous space $L(8,3)$ has a dependence on the observer position, which can be parameterised by the distance ρ as discussed above. The variability of the ensemble average with respect to ρ is shown as the grey band. The average over the interval $\rho \in [0, \pi/4]$ is plotted as the full curve. For most values of $\Omega_{\mathrm{tot}} < 1.2$ the power in the large scale correlation is indeed lower than for the simply-connected manifold $\mathbb{S}^3$ since the values are smaller than one. An even stronger suppression of large scale power is, however, revealed by the homogeneous space $N3$ for $\Omega_{\mathrm{tot}} > 1.07$.

The grey band in fig. 4a does not betray which values of the parameter ρ lead to the strongest suppression of power, that is, where the most probable observer positions occur. This information is provided by fig. 4b where for the space $L(8,3)$ the normalised power $\frac{S_{\mathcal{M}}(60^\circ)}{S_{\mathbb{S}^3}(60^\circ)}$ is shown in dependence on ρ and Ω_{tot}. Since the observer dependence is one-dimensional for the space $L(8,3)$, the observer variability is exhaust in this topology. Very low values of power are observed close to $\Omega_{\mathrm{tot}} \simeq 1.13$ and $\rho \gtrsim 0.6$. Comparing these values for ρ with the Voronoi domains shown in fig. 3, it is obvious that the best observer position belongs to the cubic Voronoi domain with $\rho = \frac{\pi}{4}$. The observer position belonging to the lens shaped domain ($\rho = 0$) is much worse than that of the cubic domain. The observation that more symmetrical domains suppress the large scale CMB power better than asymmetrical domains, is claimed in [41] where the expression "well proportioned" universes is coined. Well proportioned domains possess in all directions approximately equal extensions, whereas oddly proportioned spaces extend in some directions much more than in others. The analysis of the $L(8,3)$ space demonstrates that this rule seems to be valid even for a single manifold provided it is inhomogeneous. Therefore, it would be premature to exclude lens spaces, in general, as

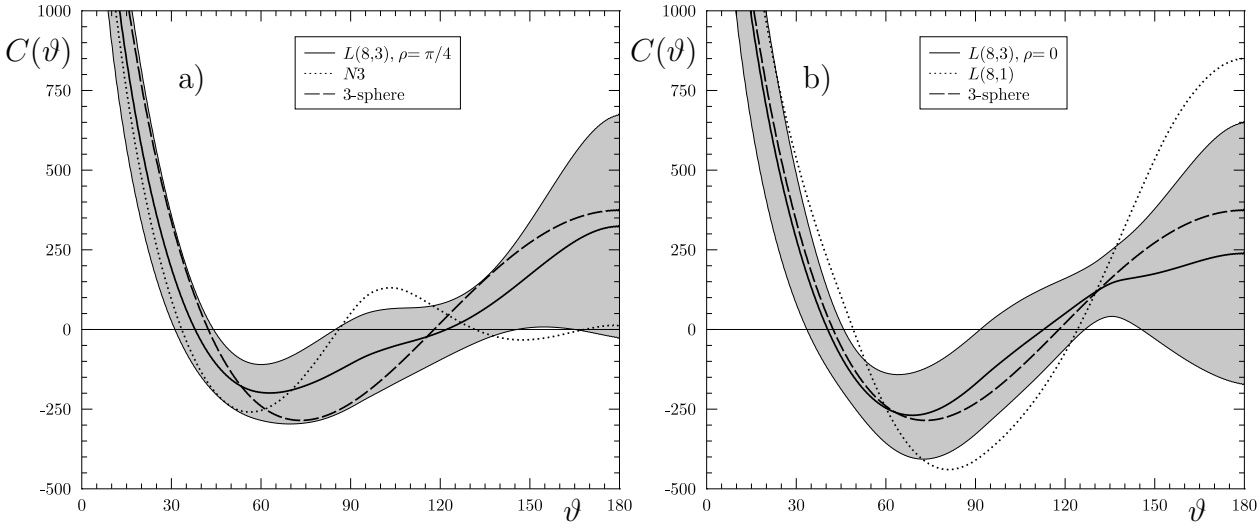

Figure 5. In panel a) the 2-point correlation functions $C(\vartheta)$ for the manifolds $L(8,3)$ with the observer at $\rho = \pi/4$ ($\equiv N2$), $N3$, and $\mathbb{S}^3$ for $\Omega_{\text{tot}} = 1.13$ are displayed. Panel b) shows $C(\vartheta)$ for the manifolds $L(8,3)$ with the observer at $\rho = 0$ ($\equiv N2$), $L(8,1)$ and $\mathbb{S}^3$. The 1-σ standard deviation of the cosmic variance is pictured as grey band for the inhomogeneous $L(8,3)$ space.

oddly proportioned spaces with high CMB power on large angular scales. Our analysis shows that the class of inhomogeneous spaces leads to a vast number of models which could in principle represent admissible models for our Universe.

Because the $S(60°)$ statistics integrates the correlation function $C(\vartheta)$, the angular information is missing. To reveal it, several correlation functions $C(\vartheta)$ are displayed in fig. 5. The correlation function $C(\vartheta)$ is shown for the inhomogeneous $L(8,3) \equiv N2$ topological space for the two observer positions characterised by $\rho = \pi/4$ and $\rho = 0$. The first case leads to a cubic Voronoi domain (see fig. 3d) and the second to a lens shaped Voronoi domain (see fig. 3a). These are compared in figs. 5a and 5b with the cubic $N3$ space and the lens shaped $L(8,1)$, respectively. For comparison, both panels also display $C(\vartheta)$ of the simply-connected $\mathbb{S}^3$ manifold. The grey band is the cosmic variance with respect to the fixed observer position of the $L(8,3)$ space. Note, that the grey band in fig. 4a is due to the various observer positions and does not include the cosmic variance. In the case of the cubic Voronoi domains (fig. 5a), the correlation function $C(\vartheta)$ of $N3$ is almost contained within the cosmic variance of the $L(8,3)$ space with $\rho = \pi/4$. For the lens shaped Voronoi domains, the difference is more pronounced as revealed by fig. 5b. The amplitude of $C(\vartheta)$ of the $L(8,1)$ space exceeds that of the $\mathbb{S}^3$ manifold for most angles ϑ.

The suppression of power at large angular scales can also be studied by the angular power spectrum C_l which is related to $C(\vartheta)$ by eq. (55). The large scale suppression is revealed by small values of C_l for small l. For larger values of l, the differences

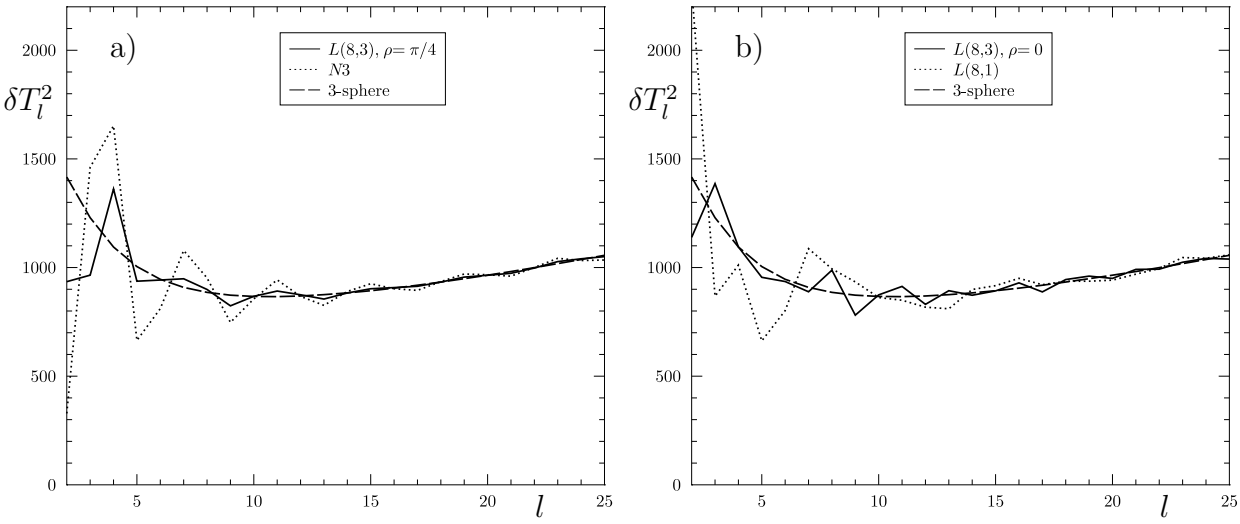

Figure 6. The angular power spectra $\delta T_l^2 = l(l+1)C_l/(2\pi)$ corresponding to the 2-point correlation functions $C(\vartheta)$ shown in fig. 5 are displayed. The spectra δT_l^2 are plotted in units $[\mu\mathrm{K}^2]$.

due to the topological signatures vanish. Most interesting is the quadrupole moment C_2. For the correlation functions $C(\vartheta)$ which are shown in fig. 5, the corresponding angular power spectra $\delta T_l^2 = l(l+1)C_l/(2\pi)$ are plotted in fig. 6. The quadrupole suppression of the cubic Voronoi domains compared to the $\mathbb{S}^3$ space is obviously visible in fig. 6a. An extreme suppression is observed for the $N3$ space due to the absence of the eigenmodes with $\beta < 5$, see eq. (58) and table 1. As fig. 6b reveals the lens shaped Voronoi domain of $L(8,3)$ possesses a slight suppression compared to $\mathbb{S}^3$, but for $L(8,1)$ a strong enhancement of power is generated by the presence of eigenmodes with $\beta = 3$. The inhomogeneous space $L(8,3)$ has also an eigenmodes with $\beta = 3$, but the multiplicity is only one whereas it is for $L(8,1)$ threefold higher, see table 1. The differences in the amplitudes of the quadrupole moment C_2 for $L(8,3)$ which are revealed by panels a) and b), are due to the position dependent phases occurring in eq. (57).

The figs. 6a and 6b reveal that the angular power spectrum δT_l^2 for the $\mathbb{S}^3$ space is smooth whereas the non-trivial topologies possess strongly fluctuating multipoles at small values of l. This is caused by the erratic fluctuating multiplicities in the case of the non-trivial topologies and the smooth, monotonically increasing multiplicities for $\mathbb{S}^3$ (see table 1).

Let us now turn to a distinct feature visible in figs. 4a and 4b. At a total energy density $\Omega_{\mathrm{tot}} = 1.208$, a spike towards higher values of $\frac{S_{\mathcal{M}}(60^\circ)}{S_{\mathbb{S}^3}(60^\circ)}$ is present which occurs in all considered topologies. This is due to the fact that for these cosmological parameters, the distance τ_{SLS} of the observer from the surface of last scattering is $\tau_{\mathrm{SLS}} \approx \pi/2$. In

this special case antipodal points on the sky having a distance $\tau_{\rm SLS} = \pi/2$ are identified and have thus the same intrinsic temperature fluctuations. Although this antipodal symmetry is not observed, it is nevertheless worthwhile to discuss its implications. This does not mean that the antipodal symmetry is perfectly mirrored on the CMB sky, since the CMB signal is composed of several contributions with different properties. To illuminate this point, fig. 7 shows the main contributions separately which are computed in the tight coupling approximation using the cosmological parameters $\Omega_{\rm cdm} = 0.238$, $\Omega_{\rm b} = 0.0485$, $\Omega_\Lambda = 0.9215$, $h = 0.681$, and $n_{\rm s} = 0.961$. The computations are carried out for the projective space $\mathbb{P}^3$ which has the property that the multiplicities of even wave numbers β vanishes. This is a common property of all spherical space forms except the spherical manifolds which are determined by an group of deck transformation with odd order. For the antipodal symmetry, it is important to recognise from the relation $Y_{lm}(-\hat{n}) = (-1)^l\, Y_{lm}(\hat{n})$ that even and odd multipoles have to be considered separately. The angular power spectra δT_l^2 shown in figs. 7a-d display even multipoles as open circles and odd multipoles as full disks. Strong fluctuations of δT_l^2 occur in the total CMB signal with respect to odd and even multipoles as shown in fig. 7a. The usual Sachs-Wolfe contribution shown fig. 7b must vanish for odd multipoles because of the antipodal symmetry. The reverse behaviour occurs for the Doppler contribution where the even multipoles must vanish, see fig. 7c. This is due to the vector character of the velocities which arise as the derivative of a scalar velocity potential. The third important contribution at large angular scales is the integrated Sachs-Wolfe (ISW) contribution shown in fig. 7d which arises partly close to the surface of last scattering (early ISW) and partly on the line of sight later on (late ISW). The early ISW possesses an even-odd asymmetry as visible in fig. 7d.

The total angular power spectrum δT_l^2 shown in fig. 7a is composed of these three contributions at large angular scales. For $l < 15$ the usual Sachs-Wolfe contribution (fig. 7b) is the most important contribution, and thus the asymmetry of the total δT_l^2 is of the kind that even multipoles l dominate the odd ones. In the range $15 < l < 70$ the Doppler contribution dominates leading to a reversal of the even-odd asymmetry in the total δT_l^2, see fig. 7a. For $l > 70$ the usual Sachs-Wolfe contribution dominates again leading to a further reversal of the even-odd asymmetry. In this way the complex behaviour of the angular power spectrum δT_l^2 can be understood. Although this discussion is restricted to the special case $\tau_{\rm SLS} = \pi/2$, the numeric shows that cosmological models having values of $\tau_{\rm SLS}$ not too far from $\pi/2$ display such a behaviour. So this asymmetric behaviour survives for a large class of models.

A comparison of the projective space $\mathbb{P}^3$ with the simply-connected $\mathbb{S}^3$ can be found in fig. 7f. Since the simply-connected $\mathbb{S}^3$ has odd and even wave numbers, no even-odd asymmetry occurs in this space form. The projective space $\mathbb{P}^3$ possesses this asymmetry as discussed due to its odd wave numbers. Although there exists no spherical space form which has only even wave numbers, it is interesting to compute the angular power spectrum δT_l^2 for an artificial spectrum having only even wave numbers. The result is shown in fig. 7f, and one observes its complementary behaviour with respect to the

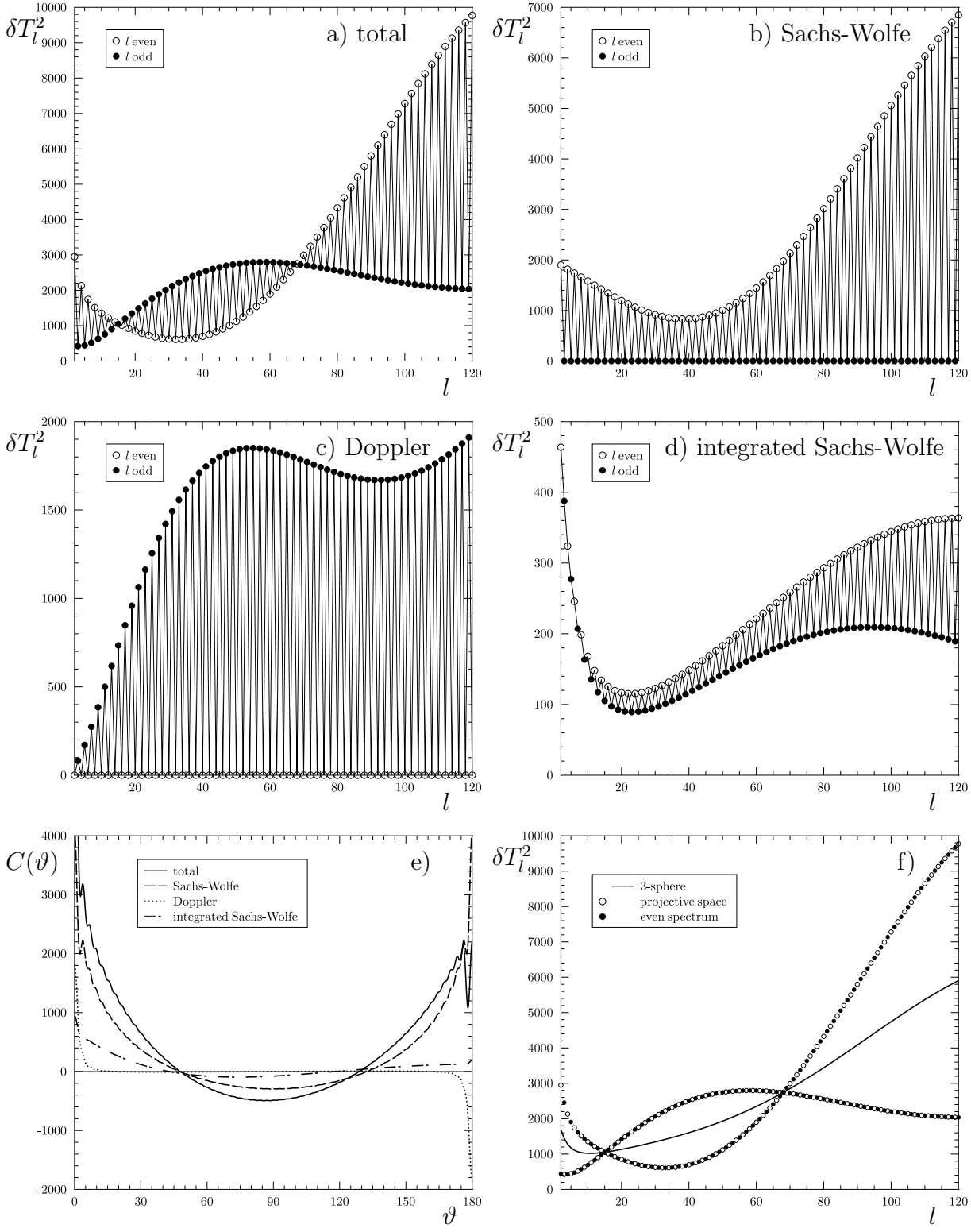

Figure 7. Panel a) shows the total contribution of the angular power spectrum δT_l^2 of the projective space $\mathbb{P}^3$ calculated in the tight coupling approximation for the cosmological parameters $\Omega_{\mathrm{cdm}} = 0.238$, $\Omega_{\mathrm{b}} = 0.0485$, $\Omega_\Lambda = 0.9215$, $h = 0.681$, and $n_{\mathrm{s}} = 0.961$. The outcome of these parameters is a distance to the surface of the last scattering $\tau_{\mathrm{SLS}} \approx \pi/2$. In panel b), c) and d) the corresponding Sachs-Wolfe, Doppler and integrated Sachs-Wolfe contributions are represented. The associated 2-point correlation functions $C(\vartheta)$ are shown in panel e). The angular power spectrum of the projective space $\mathbb{P}^3$, the 3-sphere $\mathbb{S}^3$, and calculated from the even spectrum of β are diagrammed in f).

projective space $\mathbb{P}^3$. This neatly explains why no even-odd asymmetry occurs in the case of the $\mathbb{S}^3$ space.

The even-odd asymmetry determines the behaviour of the correlation function $C(\vartheta)$ at angles around $\vartheta = 180°$. In fig. 7e the different contributions are shown separately. The asymmetry of the usual Sachs-Wolfe contribution leads to large positive values at $\vartheta = 180°$, whereas the Doppler contribution gives large negative values. This behaviour follows from eq. (55) and $P_l(-1) = (-1)^l$. Due to the dominance of the usual Sachs-Wolfe contribution at large scales, the total correlation function $C(\vartheta)$ possesses large values for $\vartheta \gtrsim 140°$. Since a low power is observed in the CMB sky at these scales, models with $\tau_{\mathrm{SLS}} \simeq \pi/2$ are unrealistic.

5. Summary and Discussion

In this paper we study spherical models of our Universe which possess spatial spaces that are multi-connected. These spaces with positive spatial curvature arise by tiling the 3-sphere $\mathbb{S}^3$ using a deck group H. We restrict attention to groups of order 8 such that the volume of the considered manifolds is $\mathrm{vol}(\mathbb{S}^3)/8 = 2\pi^2/8$. There are two such lens spaces $L(8,1)$ and $L(8,3)$, and the D_8^* manifold which is obtained by the binary dihedral group D_8^*. Furthermore, there are two cubic Platonic manifolds $N2$ and $N3$, however, it is shown that $N2$ and $L(8,3)$ are equivalent and $N3$ corresponds to D_8^*.

Such a multi-connected space can be represented by its fundamental domain which is the subset of points such that no element of $g \in H$, $g \neq e$ can operate inside the domain, but any point of the cover outside the domain can be reached by the action of H on a point inside the domain. Such a cell is called a Voronoi domain. It is the natural domain for an observer sitting at the origin of the coordinate system for which the group elements $g \in H$ are defined. If the group elements $g \in H$ are independent of the choice of the position of the observer, all observers construct the same Voronoi domain. Such manifolds are called homogeneous. On the other hand, if there is such a dependence, the shape of the Voronoi domain varies and such manifolds are called inhomogeneous. From the above manifolds, only $L(8,3) \equiv N2$ is inhomogeneous. One can construct a spatial curve along which the observer can be shifted such that at one position the lens shaped Voronoi domain emerges whereas at an other position, the cubic Platonic Voronoi domain $N2$ appears. Other positions do not lead to domains having special properties.

The important point for cosmic topology is that the statistical properties of the CMB anisotropies depend on the group elements $g \in H$ defined for an observer that sits at the origin of the coordinate system. Thus, inhomogeneous manifolds allow a much richer variety of CMB anisotropies, and the comparison with observations is much more involved. For the multi-connected spherical spaces generated by groups H of order 8, the temperature 2-point correlation function $C(\vartheta)$, eq. (54), and the multipole moments C_l, eq. (56), are computed for the CMB anisotropies. A suitable measure for the suppression of the anisotropies at large angular scales is the $S(60°)$ statistics (59) which emphasises

the unusual behaviour at scales $\vartheta \geq 60°$. The focus is put on the inhomogeneous space $L(8,3) \equiv N2$, for which a one dimensional sequence of observer positions is derived which exhaust all possibilities allowed by this inhomogeneous space. The CMB anisotropies are calculated for this sequence, and it turns out that the strongest large scale suppression occurs for the Platonic cubic Voronoi domain, which has the observer in the centre of the $N2$ cell. On the other hand, the least suppression is observed for the lens shaped domain. This is in agreement with the hypothesis that well proportioned domains give the largest suppression of power. Thus, the example of the inhomogeneous lens space $L(8,3) \equiv N2$ demonstrates that it can be premature to classify all lens spaces as not-well proportioned domains and thus uninteresting with respect to the observed CMB power suppression. Nevertheless, for $\Omega_{\text{tot}} > 1.07$, the homogeneous Platonic space $N3$ leads to an even stronger suppression of large scale CMB anisotropy than it is the case for all observer positions in $N2$.

The special case that appears when the distance τ_{SLS} to the surface of last scattering satisfies $\tau_{\text{SLS}} = \pi/2$ is studied, although the cosmological parameters are unrealistic in this case. Then the topology requires an antipodal symmetry which partly survives in the CMB anisotropies and is reflected in the $S(60°)$ statistics. It is discussed in detail how the different contributions affect the CMB signal in distinct ways as presented in fig. 7.

Acknowledgements

We would like to thank the Deutsche Forschungsgemeinschaft for financial support (AU 169/1-1). The WMAP data from the LAMBDA website (lambda.gsfc.nasa.gov) were used in this work.

References

[1] Aurich R, Lustig S, and Steiner F, *CMB anisotropy of the Poincaré dodecahedron*, Class. Quantum Grav. **22** (2005) 2061-83, arXiv:astro-ph/0412569

[2] Aurich R, Lustig S, and Steiner F, *CMB anisotropy of spherical spaces*, Class. Quantum Grav. **22** (2005) 3443-59, arXiv:astro-ph/0504656

[3] Aurich R, Lustig S, and Steiner F, *The circles-in-the-sky signature for three spherical universes*, Mon. Not. R. Astron. Soc **369** (2006) 240-248, arXiv:astro-ph/0510847

[4] Bellon M P, *Elements of dodecahedral cosmology*, Class. Quantum Grav. **23** (2006) 7029-43, arXiv:astro-ph/0602076

[5] Coleman A J, *Induced and subduced representations*, in: Group Theory and its Applications, ed. E M Loebl, Academic Press, New York 1968

[6] Coxeter H S M and Moser W O J, *Generators and relations for discrete groups*, Springer, Berlin 1965

[7] Coxeter H S M, *Regular polytopes*, Dover, New York 1973

[8] Edmonds A R, *Drehimpulse in der Quantenmechanik*, Biblographisches Institut, Mannheim 1964

[9] Einstein A, *Kosmologische Betrachtungen zur Allgemeinen Relativitätstheorie*, Sitzungsber. Preuß. Akad. Wiss. 1917, 142-152

[10] Everitt B, *3-manifolds from Platonic solids*, Topology and its Applications **138** (2004), 253-63

[11] Gausmann E, Lehoucq R, Luminet J-P, Uzan J-P, and Weeks J, *Topological lensing in spherical spaces*, Class. Quantum Grav. **18** (2001) 5155-5186,

[12] Gundermann J, *Predicting the CMB power spectrum for binary polyhedral spaces*, arXiv:astro-ph/0503014

[13] Humphreys J E, *Reflection groups and Coxeter groups*, Cambridge University Press, Cambridge 1990

[14] Ikeda A, *On the spectrum of a Riemannian manifold of positive constant curvature*, Osaka J. Math. **17** (1980) 75-93

[15] Ikeda A, *On the Spectrum of homogeneous spherical space forms*, Kodai Mathematical Journal **18** (1995) 57-67

[16] Kramer P, *An invariant operator due to F Klein quantizes H Poincare's dodecahedral manifold*, J Phys A: Math Gen **38** (2005) 3517-40

[17] Kramer P, *Harmonic polynomials on the Poincare dodecahedral 3-manifold*, J. of Geometry and Symmetry in Physics **6** (2006) 55-66

[18] Kramer P, *Platonic polyhedra tune the 3-sphere: Harmonic analysis on simplices*, Physica Scripta **79** (2009) 045008, arXiv:0810.3403

[19] Kramer P, *Platonic polyhedra tune the 3-sphere II: Harmonic analysis on cubic spherical 3-manifolds*, Physica Scripta **80** (2009) 025902, arXiv:0901.0511

[20] Kramer P, *Platonic polyhedra tune the 3-sphere III: Harmonic analysis on octahedral spherical 3-manifolds*, Physica Scripta **81** (2010) 025005, arXiv:0908.1000

[21] Kramer P, *Platonic topology and CMB fluctuations: homotopy, anisotropy and multipole selection rules*, Class. Quantum Grav. **27** (2010) 095013

[22] Kramer P, *Multipole analysis in cosmic topology*, in: Proc. Symmetries in Nature, Symposium in Memoriam Marcos Moshinsky, Mexico 2010, eds. R Jauregai, R Bijker, and O Rosas, AIP, arXiv:1009.5825

[23] Kramer P, *New spherical spaces for cosmic topology with multipole selection rules*, submitted for publication
arXiv:1011.4274

[24] Lachièze-Rey M and Luminet J-P, *Cosmic Topology*, Phys. Rep. 254 (1995) 135-214

[25] Lachièze-Rey M, *Laplacian eigenmodes for the three-sphere*, J. Phys. A: Math. Gen. **37** (2004) 5625-5634

[26] Lehoucq R, Weeks J, Uzan J-Ph, Gausmann E, and Luminet J-P, *Eigenmodes of 3-dimensional spherical spaces and their application to cosmology*, Class. Quantum Grav. **19** (2002) 4683-4708

[27] Lehoucq R, Uzan J-P, and Weeks J, *Eigenmodes of Lens and Prism Spaces*, Kodai Mathematical Journal **26** (2003) 119-136

[28] Levin J, *Topology and Cosmic Microwave Background*, Phys. Rep. 365 (2002) 251-333

[29] Luminet J-P, Weeks J R, Riazuelo A, Lehoucq R, and Uzan J-Ph, *Dodecahedral space topology as an explanation for weak wide-angle temperature correlations in the cosmic microwave background*, Nature **425** (2003) 593-5

[30] Lustig S, *Mehrfach zusammenhängende sphärische Raumformen und ihre Auswirkung auf die Kosmische Mikrowellenhintergrundstrahlung*, Verlag Dr. Hut, München, 2007, 1. Auflage

[31] Okabe A, Boots B, Sugihara K, and Chiu S N, *Spatial Tessellations: Concepts and Applications of Voronoi Diagrams*, Wiley Series in Probability and Statistics, Wiley & Sons Ltd, 2000.

[32] Risbo T, *Fourier transform summation of Legendre series and D-functions*, Journal of Geodesy **70** (1996) 383-396

[33] Roukema B F, Lew B, Cechowska M, Marecki A, and Bajtlik S, *A Hint of Poincaré Dodecahedral Topology in the WMAP First Year Sky Map*, Astron. Astrophys. **423** (2004) 821, arXiv:astro-ph/0402608

[34] Roukema B F and Kazimierczak T A, *The size of the Universe according to the Poincaré dodecahedral space hypothesis*, arXiv:1106.0727 [astro-ph.CO]

[35] de Sitter W, *Einsteins's Theory of Gravitation*, Mon. Not. R. Astron. Soc **78** (1917) 3-28

[36] Seifert H and Threlfall W, *Lehrbuch der Topologie*, Leipzig 1934, Chelsea Reprint, New York 1980
[37] Sommerville D M Y, *An introduction to the geometry of N dimensions*, Dover, New York 1958
[38] Spergel D N et al., *First Year Wilkinson Microwave Anisotropy Probe (WMAP) Observations: Determination of Cosmological Parameters*, Astrophys. J. Suppl. **148** (2003) 175-194, arXiv:astro-ph/0302209
[39] Uzan J-P, Riazuelo A, Lehoucq R, and Weeks J, *Cosmic microwave background constraints on lens spaces*, Phys. Rev. **D69** (2004) 043003, arXiv:astro-ph/0303580
[40] Weeks J, *Exact polynomial eigenmodes for homogeneous spherical 3-manifolds*, Class. Quantum Grav. **23** (2006) 6971-6988
[41] Weeks J, Luminet J-P, Riazuelo A, Lehoucq R, *Well-proportioned universes suppress CMB quadrupole*, Mon. Not. R. Astron. Soc **352** (2004), 258
[42] Wigner E P, *Group theory and its applications to the quantum mechanics of atomic spectra,* Wiley, New York 1959
[43] Wolf J A, *Spaces of constant curvature*, Publish or Perish Inc., Washington, US 1984, 5th Edition